SiF 2020 – The 11th International Conference on Structures in Fire
The University of Queensland, Brisbane, Australia, 30th November - 2nd December, 2020

MODELLING CONCRETE SLABS SUBJECTED TO LOCALISED FIRE ACTION WITH OPENSEES

Liming Jiang[1], Mhd Anwar Orabi[2], Jin Qiu[3], Asif Usmani[4]

ABSTRACT

Reinforced concrete slabs in fire have been heavily studied over the last three decades. However, most experimental and numerical work focuses on long-term uniform exposure to standard fire. Considerably less effort has been put into investigating the response to localised fires that result in planarly non-uniform temperature distribution in exposed elements. In this paper, the OpenSees for Fire framework is presented, verified against benchmark solutions, and validated against experimental tests. The thermal wrapper developed within OpenSees is then presented and used to apply localised fire exposure to the validated slab models. It is seen that the deflections produced by the localised fire exposure are less than the standard fire exposure. It is also shown that by using the damage perimeter from the concrete damage plasticity model developed for OpenSees it is possible to predict the degree of cracking in the top layer each fire model is expected to produce.

Keywords: Structures; finite element modelling; localised fire; fire tests

1 INTRODUCTION

The Open System for Earthquake Engineering Simulation (OpenSees) is a powerful open source finite element framework primarily for seismic loading [1]. Its open source nature gives it a unique extensibility and reach not enjoyed by other expensive commercial software or in-house propriety codes. This was one of the crucial reasons why it was chosen to be a research platform for simulating structure interaction with various fire scenarios such as the post-flashover fires, localised fires, traveling fire scenarios, and Computational Fluid Dynamics (CFD) results. The behaviour of concrete slabs such as tensile membrane action has been recognised by previous research when studying the global response of composite floor systems to fires and especially the progressive collapse mechanism due to fire [2]. Recently, the ability to model slabs in fire with geometric nonlinearity was added to OpenSees by introducing the geometrically nonlinear shell element NLDKGQThermal. Material degradation and damage was also incorporated by the development of a 2D plane stress formulation of the thermo-mechanical Concrete Damage Plasticity (CDP) model for use with the shell elements. In OpenSees, reinforcement could be modelled within the section abstraction as either a continuous 2-dimensional layer of plane-stress steel material, or as a layer of uniaxial steel material representing rebars in a particular orientation. This paper introduces the OpenSees approach for modelling slabs in fire, including temperature calculation, thermo-mechanical materials, section abstractions, and shell elements. Validation against experimental work from literature is presented for ambient and high-temperature scenarios. Finally, a demonstrating example regarding the response of slabs to localised fire behaviour is presented showcasing the ability of this framework to capture the effects of

[1] Dr., Deparment of Building Services Engineering, The Hong Kong Polytechnic University,
e-mail: liming.jiang@polyu.edu.hk, ORCID: https://orcid.org/0000-0001-8112-2330
[2] Mr., Deparment of Building Services Engineering, The Hong Kong Polytechnic University,
e-mail: anwar.orabi@connect.polyu.hk, ORCID: https://orcid.org/0000-0001-5083-3623
[3]Ms., Deparment of Building Services Engineering, The Hong Kong Polytechnic University,
e-mail:jinjin.qiu@connect.polyu.hk ORCID:https://orcid.org/0000-0002-0603-854X
[4]Ms., Deparment of Building Services Engineering, The Hong Kong Polytechnic University,
e-mail: asif.usmani@polyu.edu.hk, ORCID: https://orcid.org/0000-0003-2454-5737

https://doi.org/10.14264/2acf3b9

moderate fires which is different from the traditional uniform post-flashover fire scenarios. This work marks an important milestone for the OpenSees for Fire project, and is available for download here, where researchers and engineers from around the world are free to explore its features and use it for their study and research.

2 MODELLING ABSTRACTIONS IN OPENSEES FOR FIRE

2.1 Thermal action

OpenSees for Fire is equipped with a capable 3D heat transfer solver [3]. Within the heat transfer framework, the user specifies a 'heat transfer entity' and its mesh parameters, boundary conditions, and material type. There are predefined families of materials and entities covering the most common types used in structural engineering such as Hasemi's model [4]. Likewise, for boundary conditions the user may either define temperatures, heat flux, or select from a family of fire models including the SFPE localised fire, natural temperature-time curve, and hydrocarbon curve [5]. For concrete slabs under the most common standard uniform heating scenarios, one dimensional heat transfer analysis is often sufficient to produce an accurate temperature history for thermo-mechanical analysis. For localised heating regimens, a series of one-dimensional heat transfer analysis would likely produce a sufficiently detailed temperature history map for structural analysis, as was shown in [6]. Three-dimensional heat transfer analysis is often unnecessary and may be reserved for more complicated thermal exposures such as those experienced in traveling fires. The results of the heat transfer analysis can then be applied to the structural model over 15 points in a beam element or 9 points through the depth of a shell element. To represent localised fire exposure in the structural model, temperatures from the heat transfer analysis are applied over a set of individual nodes. To facilitate this process for the user, temperature data is only required over three nodes with OpenSees interpolating the temperature histories and mapping them to all nodes within the radius specified by the selected nodes via a thermal action wrapper object as shown in Figure 1. The temperature interpolation performed by the wrapper considers smooth heat flux transition between the central region and the far point as shown in [7].

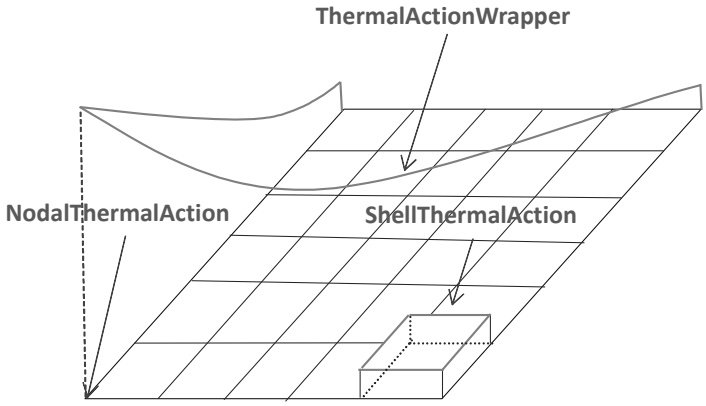

Figure 1. Thermal action wrapper in OpenSees

2.2 Shell element and section abstraction

Formerly, OpenSees for Fire was only capable of modelling slabs using plate sections with a limited number of fibres and only using a single material. That approach required at least two shell elements to represent the reinforcement and concrete layers of a typical steel reinforced concrete slab [8]. Recently, a thermo-mechanical NLDKGQ shell element was introduced to OpenSees for fire based on the work by Lu et al. [9], which enables geometric nonlinearity using updated Lagrangian approach. A layered section capable of representing slab sections with layers to represent the concrete and reinforcement at elevated temperature. As shown in Figure 2, the ShellNLDKGQThermal shell element has four nodes with six degrees of freedom and through-depth temperature profile for each node, which are interpolated for the four Gauss points to obtain section deformation and temperature distribution. Smeared steel reinforcement

is represented as a plane stress layer using uniaxial steel material oriented with respect to the element local axis as shown in Figure 2 (b). In a similar way, concrete is modelled as a plane stress layer of multi-axial Concrete Damage Plasticity (CDP) material which was developed by the authors particularly for slabs in fire as discussed in the next section.

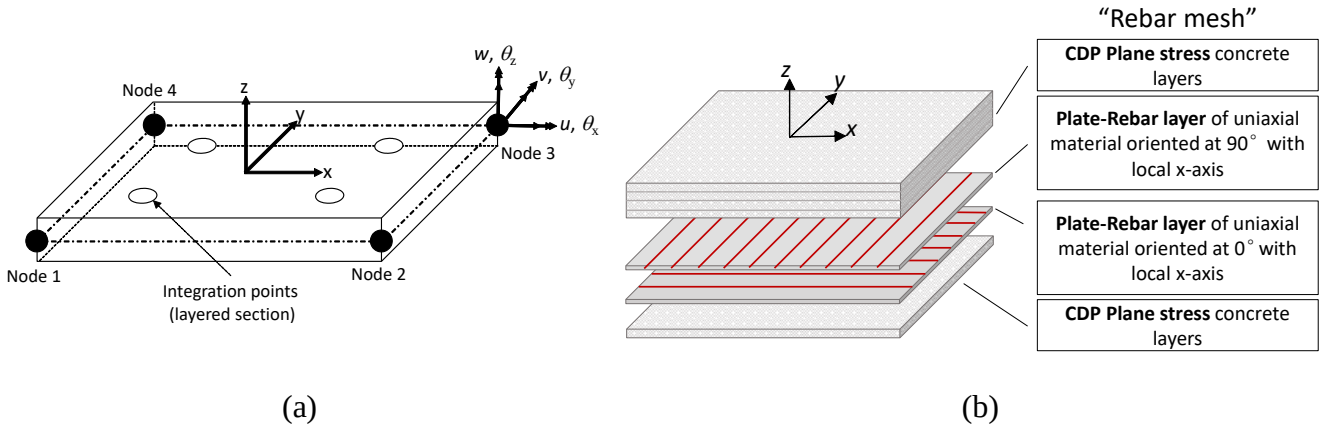

(a) (b)

Figure 2. Abstractions for modelling reinforced concrete slabs in OpenSees for Fire. (a) element definition, (b) layered shell section definition

2.3 Concrete damage plasticity

Modelling concrete in fire is a difficult task because of the potential for stress reversal, thermal degradation, and especially the damage. Modelling such phenomena requires balance between computational expense and accuracy which is exactly what the CDP model provides. CDP was first introduced by Lubliner et al. [10] and then improved by Lee and Fenves [11] who decoupled the degradation damage from the elastoplastic state determination. Since then, it has been used successfully for analysing the behaviour of concrete slabs in fire [12,13]. A plane-stress variation of the CDP based on the return-mapping algorithm developed by Lee and Fenves [14] has been adopted in this work and uses the yield surface shown in Figure 3. Concrete thermo-mechanical properties based on the provisions of the EN 1992-1-2 [15] are incorporated with the damage plasticity formulation, with inclusion of load induced thermal strains as provided by Le et al. [16].

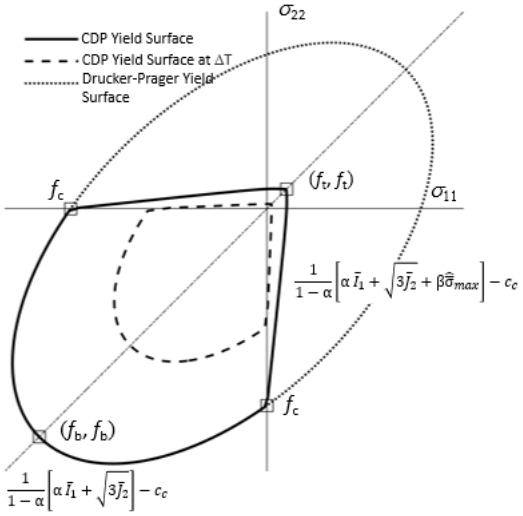

Figure 3. CDP and Drucker-Prager yield surfaces and degradation of CDP yield surface with temperature

3 VERIFICATION AND VALIDATION

3.1 Verification of geometric nonlinearity

Geometric nonlinearity is one of the primary complications that arise within nonlinear thermo-mechanical analysis. High axial forces due to expansion coupled with large deflections result in second order effects that may dominate the behaviour. These second-order effects are clearly evident in tensile-membrane action which occurs when a slab reaches a deformation in the same order of its thickness as demonstrated experimentally by Nguyen and Tan [17]. In this section, the aforementioned developments are verified against analytical solutions for a benchmark geometrically nonlinear elastic problem. The cantilever shown in Figure 4 (a) is modelled identically in OpenSees using corotational beam elements and both linear and nonlinear shell elements. The thin beam is tested for both mechanical loading alone and thermo-mechanical loading. In the first case, it is only subjected to an edge mechanical load *P*. In the second, it is also subjected to a uniform thermal gradient with bottom temperature of 1000 °C and top temperature of 0 °C. The vertical displacement of both cases is plotted in Figure 4 against the analytical solution and prediction by a beam element. In both cases, the linear shell elements give poor predictions compared to the nonlinear shell elements which agree very well with their respective benchmarks.

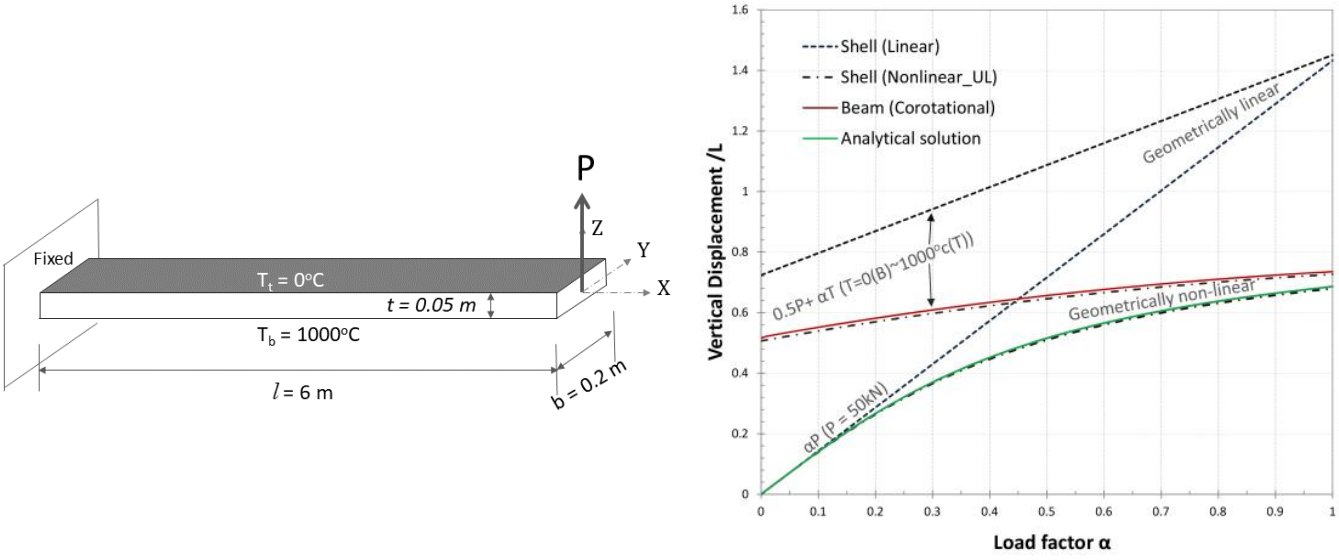

(a) (b)

Figure 4. Verification of geometric nonlinearity (a) problem definition, (b) comparison of results

3.2 Validation against experimental results

A series of simply supported full-scale slab specimens were tested in New Zealand under uniform vertical load and three hour exposure to the ISO 834 standard fire [18]. Specimen D147 from [18] was modelled in OpenSees and is compared to the observed results and numerical predictions made by other researchers [13,19]. The slab was simply supported and had a foot print and thickness of 4.3 m × 3.3 m and 100 mm respectively. It was loaded with a uniform load of 5.4 kN/m^2 and then heated from the bottom for three hours. The concrete had a compressive strength of 37 MPa, and was modelled as having a tensile strength of 4 MPa and a Young's modulus of 22.2 GPa. The reinforcement was a mesh of D147 cold formed bars with a yield strength of 565 MPa and had a 25 mm thick concrete cover. The bars were 8.7 mm in diameter and were spaced at 300 mm. One dimensional heat transfer analysis produced highly representative temperatures as shown in Figure 5 (a). The central deflection predictions by OpenSees showed an earlier 'failure' than the experiment as marked by the onset of runaway deflection and thus termination of the analysis. The results compare very well with the experimental observations and other numerical predictions up to about the termination of the analysis as shown in Figure 5 (b). Slab HD12 from the same experimental

series had the same dimensions, load, and thermal exposure. The reinforcement, however, had a larger diameter of 12 mm and was more densely spaced at 200 mm. Moreover, while the rebars in D147 were cold drawn, those in HD12 were hot rolled and had a yield stress of 468 MPa. The higher reinforcement ratio, ductility of the HD12 bars as well as the better-property retention of hot rolled steel at high temperatures contributed to the lower deflection of the slab at the end of the fire loading as shown by both the experimental results and numerical prediction presented in Figure 6 (a). Figure 6 (b) shows the predictions for traction vectors across the thickness of slab D147 at around two hours of heating with a clear compressive ring on the perimeter and a tensile central region as would be expected [20].

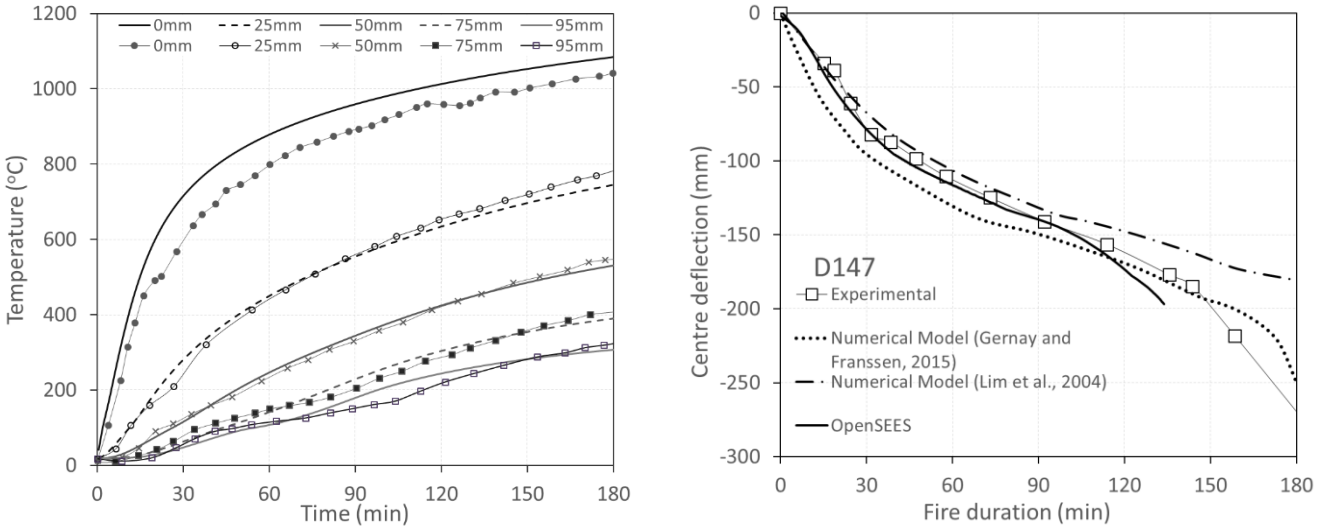

(a) (b)

Figure 5. Comparison between experimental results and numerical predictions (a) Temperature, (b) central deflection

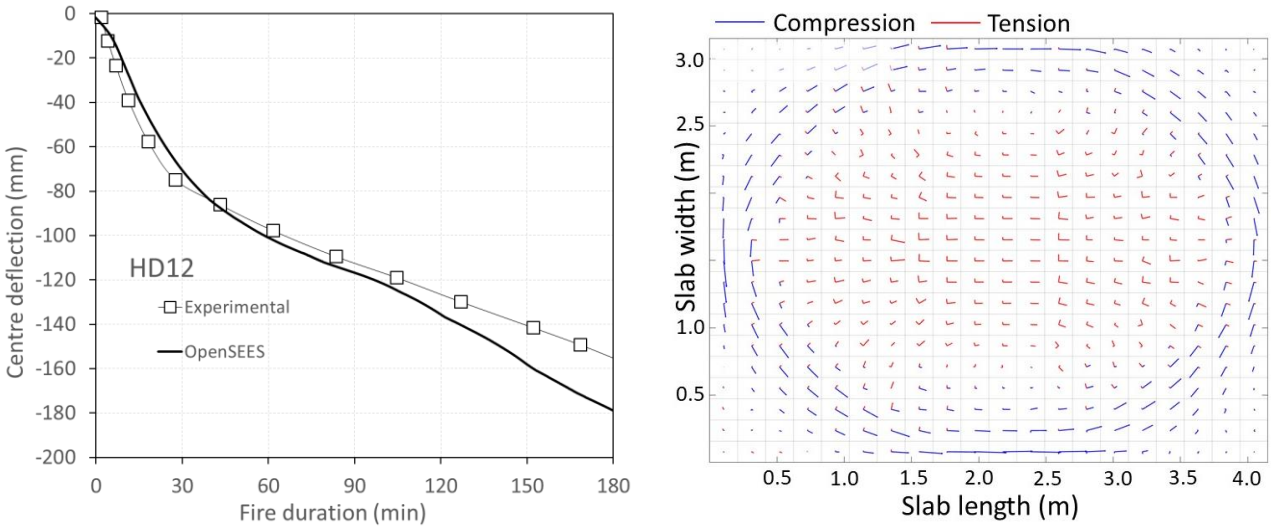

(a) (b)

Figure 6. Numerical prediction for (a) deflections of slab HD12, and (b) traction vectors in principal space for slab D147

4 MODELLING LOCALISED FIRE

4.1 Fire scenario

To demonstrate OpenSees capabilities in modelling localised fire, two localised fire scenarios were considered and applied to the validated thermomechanical models for slabs D147 and HD12. The first fire

scenario was a modified localised fire with a heat release rate of 1.127 MW validated by the localised fire test with smoke layer [4,21], and the second was a EC1 localised fire but with an increased heat release rate of 2 MW (no smoke layer modification). Both of these scenarios were run to simulate a 30-minute fire as would be consistent with short-term localised fires in building structures. The fire scenarios were applied to a three-dimensional heat transfer model to produce thermal histories for the thermo-mechanical model. The temperature profile at three points was extracted from the heat transfer model corresponding to a point at the centre of the slab, half-way to the corner, and the corner point. The temperature profiles were then applied in the thermo-mechanical model via the thermal action wrapper discussed in section 2.1 which produced an interpolated three-dimensional temperature distribution to all shell elements within the slab. The temperature distribution at the bottom of the slab after 30 minutes of heating is shown for each fire scenario in Figure 7. It is clear from this figure that the 2 MW fire without the smoke layer would produce a larger zone with the maximum temperature but with more special discrepancy as evident by the cold edges as seen in Figure 7.

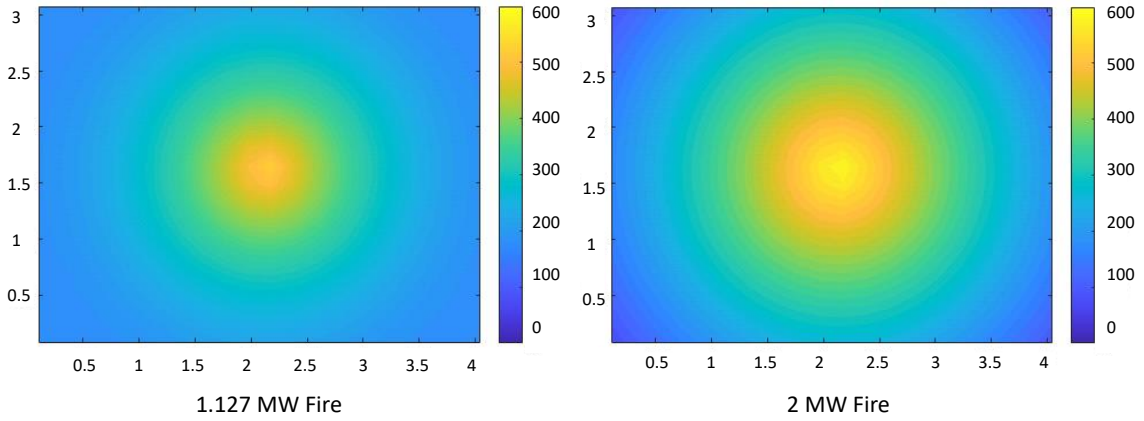

Figure 7. Layer temperature distribution near the exposed surface after 30 minutes of heating

4.2 Deflection

Thermo-mechanical analysis was performed for both slab D147 and HD12. The central deflection up to 30 minutes of heating is reported in Figure 8 (a) and (b) for specimen D147 and HD12 respectively. The experimental deflections and the deflections predicted by OpenSees for ISO 834 fire are also shown in the figure. In all cases, ISO 834 fire produces the highest deflections. This is to be expected because the entire slab is subjected to elevated temperatures that are significantly higher than the applied localised fires which heat the slabs less evenly and less severely. It is interesting to see that in this early stage of heating specimens show very similar levels of deflection for each applied fire scenario. This is because during the early stages of a fire, thermal expansion is the dominant factor governing deflection and the increments of temperature near the exposed surfaces in early period of heating are similar. The level of deflection observed for a 1.127 MW is less than the deflection observed under the 2 MW fire, which also produces less deflections than the ISO 834 fire at the end of the 30 minutes heating window. Note that the earlier stage of deflection development is overestimated for the localised fire because the model assumes the fire immediately reaches its peak heat fluxes as a steady state.

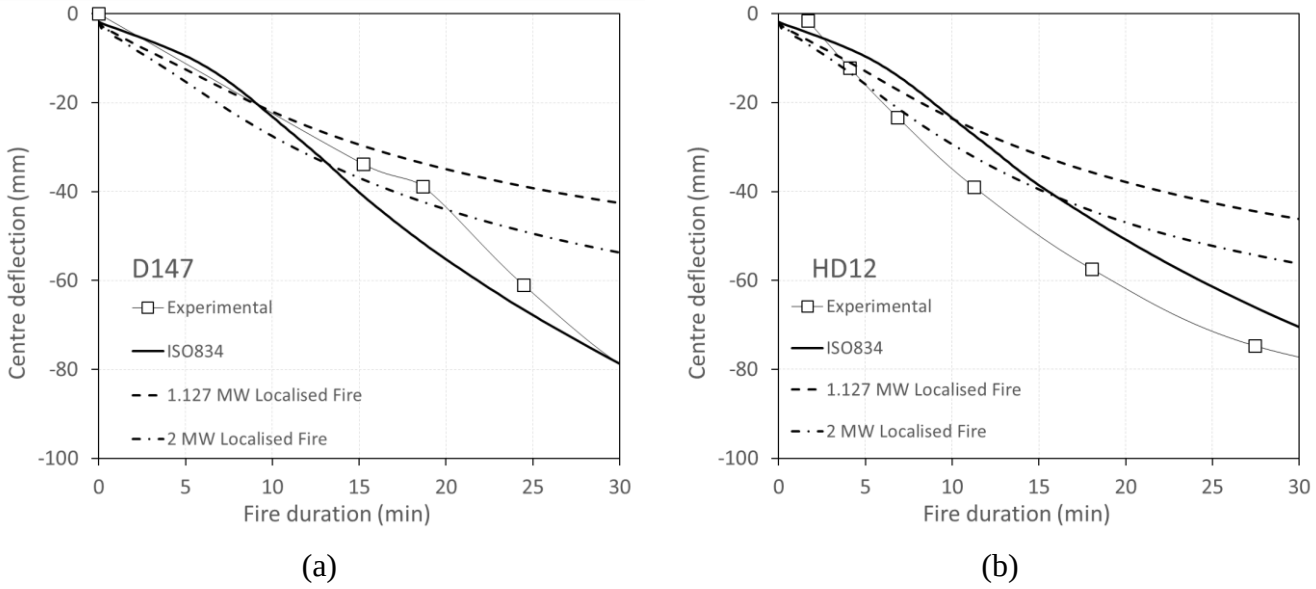

Figure 8. time-deflection curves for 30 minutes localised fire and standard fire exposure for (a) slab D147, and (b) slab HD12

4.3 Damage

It was mentioned in section 3.2 and shown in Figure 5 (b) that a compressive ring encompassing a tensile membrane region forms in the specimens by the end of the heating. By plotting the tractions in slab HD12 at the 30 minutes mark for each fire scenario in Figure 9 a clear pattern emerges. The localised fire scenarios produce less vertical deflection and heat the slab less severely and less evenly, which results in the emergence of the compression ring in the perimeter of the slab and the beginning of tensile action in the interior of the slab. As the centre of the slab is still the focal point of the heating, the midpoint is expanding relative the perimeter which puts it in compression. It is expected that if the localised fire is allowed to burn for longer, then the slab would go into full tensile membrane action. The pattern presented by the ISO 834 at 30 minutes is close to tensile membrane action even with limited vertical deflection of less than the slab thickness, which presents with a still-forming compressive ring supporting a developing central tensile region. The tractions for specimen D147 show the same pattern as those discussed for each fire scenario.

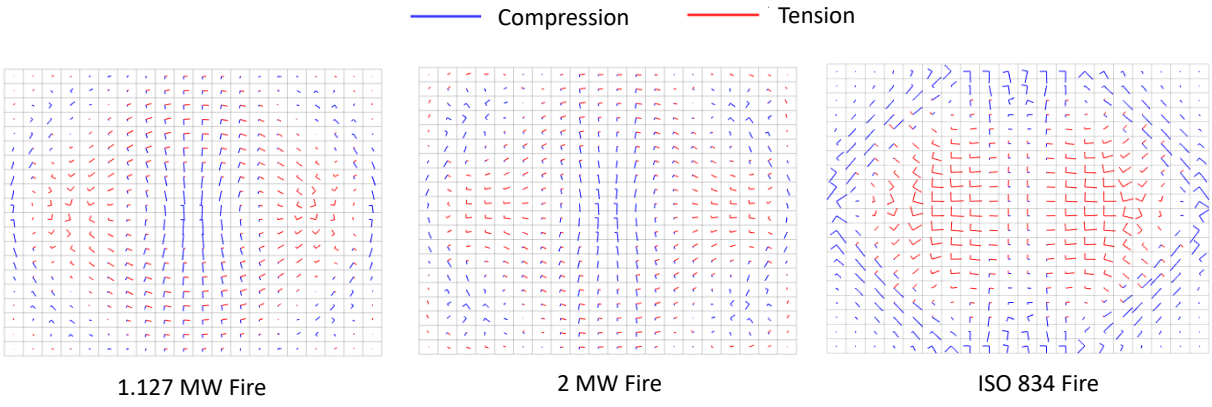

Figure 9. Tractions in slab HD12 after 30 minutes of fire exposure for each different fire scenario

The tensile damage variable D_t is shown for the top layer of slab D147 in Figure 10. The damage variable in this layer indicates the degree of surface cracking expected with $D_t = 1$ meaning the concrete is cracked and $D_t = 0$ indicating it is still intact. The ISO 834 fire predicts the most severe damage with the corners and a central strip across the short direction being fully cracked. This is consistent with the restraint provided to the slab preventing it from moving vertically at the perimeter, and with the longer direction being more flexible than the shorter direction. Similar damage is seen when the slab is subjected to the 2

MW localised fire, but to a lesser extent particularly in the middle of the slab. The 1.127 MW fire produces high tensile damage only in the corners with almost no damage across the short span in middle of the slab.

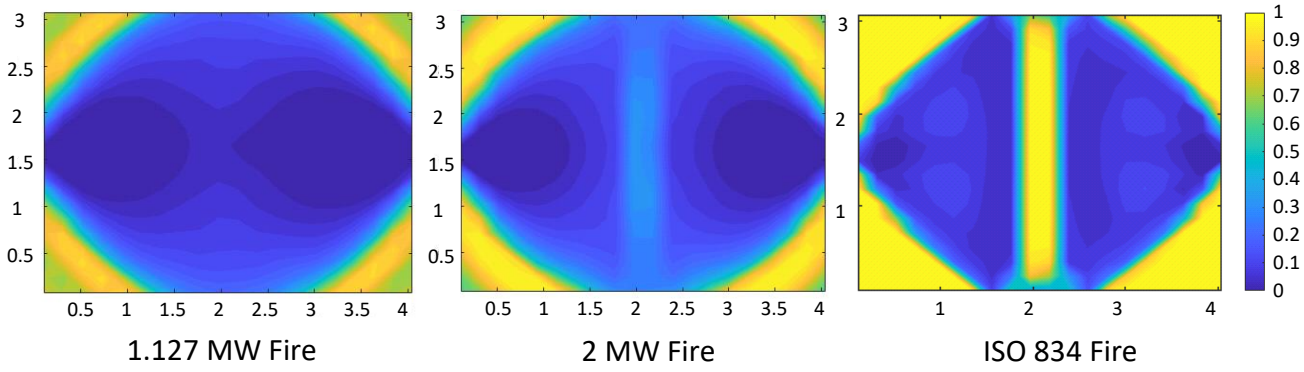

Figure 10. Tensile damage parameter D_t in top layer of D147

5 CONCLUSIONS

The OpenSees for Fire capabilities for representing concrete slabs under uniform and localised fire were presented. Validations against analytical solutions of a cantilever beam subject to thermal gradient show that the shell elements developed capture geometric nonlinearity well in thermo-mechanical analysis. Further validation against fire tests on slabs has also shown agreeable results. When subjected to two different intensities of localised fire as measured by their heat release rate, the model also produces the expected outcomes. Even the more severe localised fire with a heat release rate of 2 MW predicts lower deflections than an ISO 834 fire after 30 minutes of exposure. The tractions produced by the model show that the localised fires produce tractions that are approaching tensile membrane action as found in standard fire tests. By exporting the damage variable D_t from the CDP material in OpenSees it is possible to visualise potential top-surface cracks. The damage produced by the 1.127 MW fire is concentrated at the corners but indicating that cracks in the span may not necessarily develop after 30 minutes exposure to this fire. The 2 MW fire and the ISO 834 fire on the other hand produce prominent damage patterns with severe damage over the corners and across the short span in the middle of the slab. The work presented in this paper is to demonstrate the modelling of floor slabs in real fire behaviour with the thermo-mechanical model in OpenSees where the fire is generated as per engineering models (EC1) or CFD fire models representing real fires including the smoke layer. The fire induced damage patterns of slabs in these localised fire scenarios provides a more complete estimation of fire impact in addition to the uniform fire exposure defined by the standard fire curve.

REFERENCES

1. F. McKenna, Object-oriented finite element programming: frameworks for analysis, algorithms and parallel computing, University of California, Berkeley, 1997.
2. I. Burgess, M. Sahin, Tensile Membrane Action of Lightly-reinforced Rectangular Composite Slabs in Fire, Structures. 16 (2018) 176–197. https://doi.org/10.1016/j.istruc.2018.09.011.
3. Y. Jiang, Development and application of a thermal analysis framework in OpenSees for structures in fire, The University of Edinburgh, 2012.
4. T. Wakamatsu, Y. Hasemi, K. Kagiya, D. Kamikawa, Heating Mechanism of Unprotected Steel Beam Installed Beneath Ceiling and Exposed to a Localized Fire : Verification using the real-scale experiment and effects of the smoke layer, in: Fire Saf. Sci. Seventh Int. Symp., 2003: pp. 1099–1110.
5. M.A. Orabi, A.A. Khan, A. Usmani, An Overview of OpenSEES for Fire, in: Proc. 1st Eurasian Conf. OpenSEES OpenSEES Days Eurasia, Hong Kong, China, n.d.
6. L. Jiang, S. Chen, A. Usmani, Feasibility of dimensionally reduced heat transfer analysis for structural

members subjected to localised fire, Adv. Struct. Eng. 21 (2018) 1708–1722. https://doi.org/10.1177/1369433218754334.

7. L. Jiang, Development of an integrated computational tool for modelling structural frames in fire considering local effects, University of Edinburgh, 2015.
8. J. Jiang, P. Khazaeinejad, A. Usmani, Nonlinear analysis of shell structures in fire using OpenSees, (2012).
9. X. Lu, L. Xie, H. Guan, Y. Huang, X. Lu, A shear wall element for nonlinear seismic analysis of super-tall buildings using OpenSees, Finite Elem. Anal. Des. 98 (2015) 14–25. https://doi.org/10.1016/j.finel.2015.01.006.
10. J. Lubliner, J. Oliver, S. Oller, E. Oñate, A plastic-damage model for concrete, Int. J. Solids Struct. 25 (1989) 299–326. https://doi.org/10.1016/0020-7683(89)90050-4.
11. J. Lee, G.L. Fenves, Plastic-damage model for cyclic loading of concrete structures, J. Eng. Mech. 124 (1998) 892–900. https://doi.org/10.1061/(ASCE)0733-9399(1998)124:8(892).
12. N. Wahid, L.A. Bisby, Modelling the deflection response of reinforced concrete flat slabs during heating, in: 15th Int. Conf. Fire Sci. Eng. (Interflam 2019), 2019.
13. T. Gernay, J.M. Franssen, A plastic-damage model for concrete in fire: Applications in structural fire engineering, Fire Saf. J. 71 (2015) 268–278. https://doi.org/10.1016/j.firesaf.2014.11.028.
14. J. Lee, G.L. Fenves, Return-mapping algorithm for plastic-damage models: 3-D and plane stress formulation, Int. J. Numer. Methods Eng. 50 (2001) 487–506. https://doi.org/10.1002/1097-0207(20010120)50:2<487::AID-NME44>3.0.CO;2-N.
15. British Standards Institution, Eurocode 2 - Design of concrete structures Part 1-2: Structural fire design, (2004).
16. Q.X. Le, J.L. Torero, V.T.N. Dao, Understanding the effects of stress on the coefficient of thermal expansion, Int. J. Eng. Sci. 141 (2019) 83–94. https://doi.org/10.1016/j.ijengsci.2019.05.016.
17. T.T. Nguyen, K.H. Tan, Ultimate load of composite floors in fire with flexible supporting edge beams, J. Constr. Steel Res. 109 (2015) 47–60. https://doi.org/10.1016/j.jcsr.2015.03.004.
18. L. Lim, C. Wade, Experimental Fire Tests of Two-Way Concrete Slabs, 2002.
19. L. Lim, A. Buchanan, P. Moss, J. Franssen, Numerical modelling of two-way reinforced concrete slabs in fire, 26 (2004) 1081–1091. https://doi.org/10.1016/j.engstruct.2004.03.009.
20. N.S. Zhang, G.Q. Li, A new method to analyze the membrane action of composite floor slabs in fire condition, Fire Technol. 46 (2010) 3–18. https://doi.org/10.1007/s10694-009-0086-8.
21. L. Jiang, Y. Zhang, Z. Zhang, A. Usmani, Thermal analysis infrastructure in OpenSees for fire and its smart application interface towards natural fire modelling, Fire Technol. (2020 in-process).